Annealing effects on structural and transport properties of rf-sputtered CoFeB/MgO/CoFeB magnetic tunnel junctions

Chando Park,[a] Jian-Gang Zhu, Matthew T. Moneck, Yingguo Peng, and David E. Laughlin
Data Storage Systems Center, Carnegie Mellon University, Pittsburgh, Pennsylvania 15213

(Presented on 31 October 2005; published online 19 April 2006)

Annealing effects on the structural and transport properties of sputtered CoFeB/MgO/CoFeB magnetic tunnel junctions deposited on SiO_2/Si were investigated. At the as-deposited state, the CoFeB was amorphous at the CoFeB/MgO interface. High-resolution transmission electron microscope image clearly shows that after annealing at 270 °C for 1 h, crystallization of amorphous CoFeB (three to four monolayers) with lattice matching to MgO (100) occurred locally at the interface between MgO and CoFeB, producing a magnetoresistance (MR) around 35%–40%. After annealing at 360 °C for 40 min, the MR increased to 102%. The increase in the MR with annealing is attributed to the complete formation of (100) crystalline structure of CoFeB well lattice matched with the (100)-oriented MgO barrier. The bias voltage dependence of the MR shows a consistent correlation with each CoFeB/MgO interface. © *2006 American Institute of Physics*.
[DOI: 10.1063/1.2165141]

Magnetic tunnel junctions (MTJs), in which spin-dependent tunneling occurs, have shown a high magnetoresistance (MR) effect (i.e., the resistance change due to the applied magnetic field) and have become the most promising structure for the application of magnetoresistive devices such as magnetic random access memory (MRAM), magnetic read heads, and magnetic sensors.[1] In order to obtain better performance for these devices, it is important that the MR effect is large, because this will enable the devices to be operated at higher speeds with a greater signal-to-noise ratio.[2]

Based on first-principle electronic structure calculations, MTJs with the structure of Co, CoFe, or Fe (100)/MgO (100)/Co, CoFe, or Fe (100) were predicted to produce much higher MR than conventional MTJs with an amorphous AlO_x tunnel barrier.[3–5] Parkin *et al.* and Yuasa *et al.*[6,7] have obtained high MR experimentally using a MgO tunnel barrier, confirming the prediction. Recently, MTJs consisting of CoFeB/MgO/CoFeB have been fabricated and have also shown large MR at room temperature.[8,9] They showed that high MR in CoFeB/MgO/CoFeB MTJs could be obtained only after an annealing treatment. However, annealing effects on the microstructure of these MTJs are not clear yet, even though speculation on the effect of annealing has been suggested.

In this paper, we present the experimental results of our investigation of annealing effects on the structural and transport properties of sputtered CoFeB/MgO/CoFeB magnetic tunnel junctions.

Single-layer thin films of MgO and layered stacks of Ta 10 nm/$Pt_{38}Mn_{62}$ 30 nm/$Co_{90}Fe_{10}$ 1.5 nm/$Co_{60}Fe_{20}B_{20}$ 2.5 nm/MgO 2–3 nm/$Co_{60}Fe_{20}B_{20}$ 5 nm/Ta 5 nm were deposited on 7059 glass and oxidized silicon substrates by using a rf/dc sputtering system. All of the junctions were patterned by photolithography and ion-beam etching. The junction sizes varied from 1×1 to 8×8 μm^2. The tunnel barrier layer was formed by rf sputtering from MgO target. For the annealing at 360 °C, the samples were annealed for 40 min using rapid thermal annealing (RTA) without the application of magnetic field and subsequently annealed at 270 °C for 60 min in a vacuum under a magnetic field of 1000 Oe to induce a unidirectional exchange field (H_{ex}) of PtMn/CoFe/CoFeB-pinned layer. The phase identity of the films was investigated by x-ray diffraction (XRD). The interface of the films was investigated by high-resolution transmission electron microscopy (HRTEM), and the magnetic properties were measured at room temperature using a vibrating-sample magnetometer (VSM). The MR transfer curve was measured using a four-point probe measurement system with fields up to 3000 Oe.

To obtain a MgO barrier with appropriate texture, the crystallinity of the single-layer MgO films was investigated by varying deposition pressure. The XRD patterns for the single-layer MgO films deposited at different pressures on 7059 glasses are shown in Fig. 1. The thicknesses of all the films were estimated to be 30 nm. The intensities of the XRD patterns of the films are different depending on the deposition pressure. The MgO film deposited at 5 mT produced a strong XRD intensity, suggesting a relatively large grain size. It turned out that the grain size of the film deposited at 5 mT was about 25 nm, as measured by TEM. The XRD patterns revealed only the (200) peak, suggesting that highly (100)-oriented films were formed. The degree of film orientation in the [200] was investigated by rocking curve measurement, as shown in the inset. A rocking curve full width at half maximum (FWHM) value of 7.7° was observed for (200) MgO films deposited at the pressure of 5 mT, indicating a good textured MgO film. Annealing treatments up to 380 °C did not produce a significant change in (200) peak intensity. Therefore, the crystallinity of the MgO film depends critically on the deposition condition. For the rest of the results, all MgO films were deposited at 5 mT.

[a]Electronic mail: chando@andrew.cmu.edu

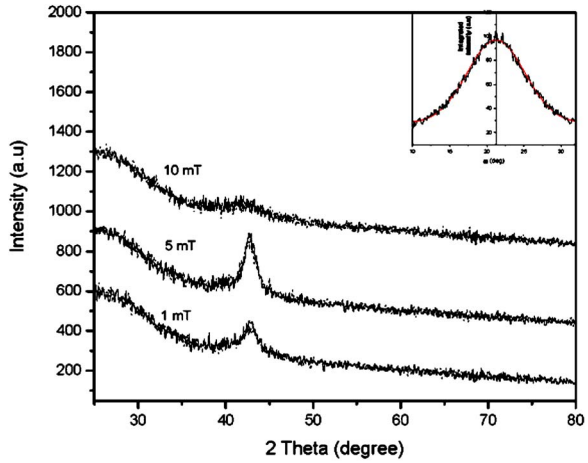

FIG. 1. XRD patterns of the films deposited at different deposition pressures. Rocking curve of the film deposited at 5 mT was shown in the inset located in the upper corner of the figure.

Figure 2 shows the measured MR curves and corresponding magnetic hysteresis (MH) loops of the junction structures of Ta 10 nm/PtMn 30 nm/CoFe 1.5 nm/CoFeB 2.5 nm/MgO 2.2 nm/CoFeB 5 nm/Ta 5 nm film stacks, (a) as-deposited, (b) annealed at 270 °C for 60 min, and (c) annealed at 360 °C for 40 min. The insertion of 1.5 nm CoFe film between PtMn and bottom CoFeB layer was used to enhance the exchange coupling because the coupling between PtMn and CoFeB did not produce a strong exchange bias. The MR curve of the as-deposited MTJ shows a relatively small MR (~20%) and a typical MR curve of a trilayer structure due to the fact that no exchange bias was induced. The exchange bias field increased with increases in the annealing temperature. The MR was also increased drastically by the annealing and a MR ratio of 102% was obtained, even though a perfect antiparallel state was not achieved during field sweeping, as indicated in Figs. 2(b) and 2(c). The MH loops contain two subloops for top CoFeB and bottom CoFeB coupled with CoFe. The MH loop of bottom CoFeB coupled with CoFe continuously changed when the field swept from positive to negative, while that of top CoFeB changed sharply. Therefore, the parallel state could be achieved easily at a high field; however, the perfect antiparallel state could not be achieved due to the continuous change of magnetization in bottom CoFeB/CoFe especially when the external field swept from positive to negative. Note that the coercivity of the free layer increased with annealing (from ~3 to ~40 Oe), which can be seen as an indication of the crystallization of the CoFeB layer. The resistance of MTJ annealed at 360 °C (~100 kΩ μm^2) is little higher than that of the as-deposited MTJ (~80 kΩ μm^2), indicating a small change of crystallinity in MgO barrier. The MR of the MTJ annealed at 360 °C is much higher than that of the MTJs as-deposited and annealed at 270 °C. In order to see the annealing effect on MgO barrier itself, we did annealing experiments on single-layer MgO films and analyzed them with XRD and TEM. It turned out that MgO films became dense (reduced in lattice constant) after annealing below 400 °C, but with no obvious change in microstructure. This suggests that there is little annealing effect on MgO barrier itself, thus the reason for the increase in the MR, we believe, is caused by the change of the CoFeB structure at the CoFeB/MgO interface before and after annealing. The increase of MR with annealing temperature is partly due to the better magnetic alignment brought about by the increase in magnetic coupling between PtMn and bottom CoFeB/CoFe after high-temperature annealing.

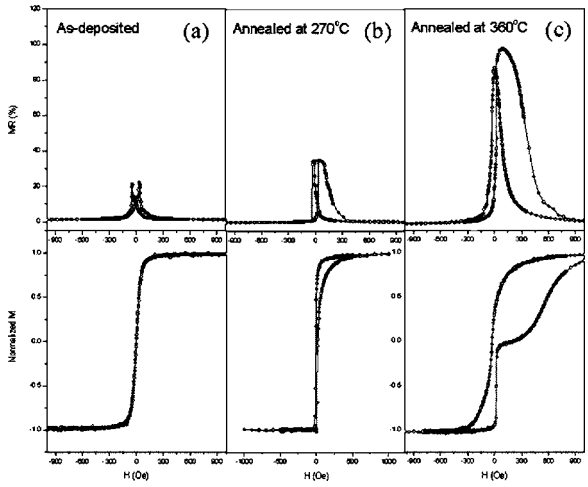

FIG. 2. Magnetoresistance transfer curves and MH loops of the junction structures of Ta 10 nm/PtMn 30 nm/CoFe 1.5 nm/CoFeB 2.5 nm/MgO 2.2 nm/CoFeB 5 nm/Ta 5 nm film stacks, (a) as-deposited, (b) annealed at 270 °C for 60 min, and (c) annealed at 360 °C for 40 min.

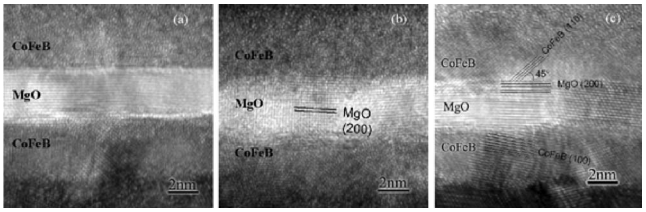

FIG. 3. High-resolution cross-sectional transmission electron micrographs of Ta 10 nm/PtMn 30 nm/CoFe 1.5 nm/CoFeB 2.5 nm/MgO 3 nm/CoFeB 5 nm/Ta 5 nm film stacks, (a) as-deposited, (b) annealed at 270 °C for 60 min, and (c) annealed at 360 °C for 40 min.

To investigate the interface in MTJs, (HRTEM) was used. The HRTEM images in Fig. 3 show the CoFeB/MgO/CoFeB interfaces for MTJs (a) as-deposited, (b) annealed at 270 °C, and (c) annealed at 360 °C. To identify the phases, we measured not only the *d* spacings from the fast Fourier transformation (FFT) of the high-resolution image but also we performed XRD measurements for single-layer CoFeB film annealed at 360 °C for 1 h. It was found that after annealing, the amorphous CoFeB transformed into crystalline CoFeB having a body-centered-cubic (bcc) crystalline structure with a lattice constant of 2.86 Å. In as-deposited MTJs, top CoFeB electrode has amorphous structures [Fig. 3(a)], but bottom CoFeB has regions containing crystalline structure. The crystalline structure in bottom CoFeB layer is probably due to the crystalline structure of CoFe, which was used to enhance the magnetic coupling between bottom CoFeB/CoFe and PtMn. Crystallization of amorphous CoFeB (three to four monolayers) with lattice matching to MgO (100) occurred locally at the interface between MgO and CoFeB after annealing at 270 °C [Fig.

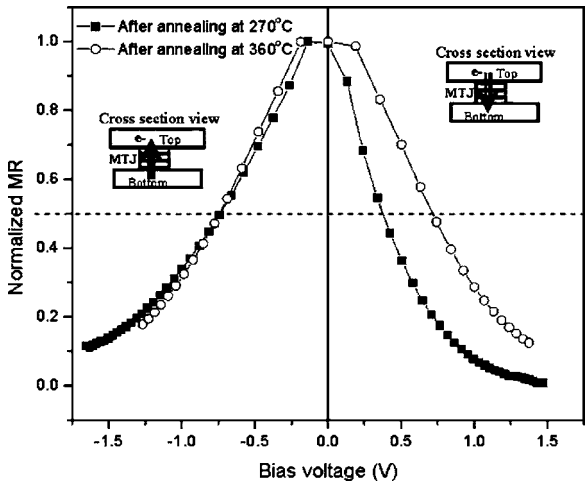

FIG. 4. Bias voltage dependence of normalized MR ratio for the MTJs annealed at 270 and 360 °C.

3(b)]. This can be easily explained by considering that the free-energy barrier is expected to be lower for nucleation occurring at the interface rather than in the bulk.[10] The top CoFeB has two interfaces, which are adjacent to amorphous Ta and crystalline MgO, respectively. After annealing at 360 °C for 40 min [Fig. 3(c)], crystallization occurred toward the CoFeB/Ta interface, which can be supported by the remaining amorphous phase in top CoFeB near the CoFeB/Ta interface. This means that crystalline MgO will further lower the energy barrier for the nucleation, resulting in crystallization starting at the interface between CoFeB and MgO. In particular, the (100) plane of MgO makes an angle of 45° with (110) plane of CoFeB, suggesting that the following orientation relation exists on MgO/CoFeB interface: MgO (100)[001]∥CoFeB (100)[110]. Therefore, the annealing changes the interface structure from amorphous CoFeB/crystalline (100) MgO to crystalline (100) CoFeB/crystalline (100) MgO, producing high MR. It is found that other orientation relationship between MgO (100) and CoFeB except for MgO (100)∥CoFeB (100) produced a low MR, even though both the top and bottom CoFeB layers were crystallized completely (these results are not shown here). These results are consistent with the theory where Zhang and Butler[5] predicted a high MR with bcc FeCo (100)/MgO (100)/bcc FeCo (100). It is important to point out that our results (obtained MR) are smaller than those reported in other works.[8,9] The reason is, we believe, as follows: (i) We did not obtain a good antiparallel alignment due to a low pinning field, as shown in Fig. 2. (ii) Bottom CoFeB was not well lattice matched with the (100)-oriented MgO barrier because the inserted CoFe layer induced the crystallization of CoFeB.

Figure 4 shows the bias voltage dependence of the normalized MR for MTJs annealed at 270 and 360 °C. As bias voltage increased, the MR decreased. Here at positive bias voltage, electrons flow from the top CoFeB electrode to the bottom CoFeB/CoFe electrode. For the MTJ annealed at 360 °C, the MR dropped to half at bias voltages of 740 and 720 mV for negative and positive voltages, respectively. However, the MR of the MTJ annealed at 270 °C dropped to half at the bias voltages of 740 and 380 mV for negative and positive voltages, respectively. This asymmetry in the bias voltage dependence of the MR of the MTJ annealed at 270 °C is due to the different structure of CoFeB at the top and bottom CoFeB/MgO interfaces, which is shown in Fig. 3(b). It is reported that the bias voltage dependence of the MR is related to the quality of the tunnel barrier and the interface structure.[11,12] As mentioned previously, the quality of the MgO barrier did not change much with annealing (~400 °C). Therefore, the interface structure is the most important feature for the bias voltage dependence of the MR of MgO MTJs. Since there is not much change in the bias voltage dependence of the MR at negative bias voltage in our case, it can be concluded that annealing does affect the interface at the top CoFeB/MgO barrier. As seen in Fig. 3, only the top electrode changes its structure because the bottom electrode already has a crystalline structure. This HRTEM analysis is consistent with the bias voltage dependence of the MR. The crystalline/crystalline interface shows much higher V_{half} than the amorphous/crystalline interface. In conclusion, we report herein on the dependence of MgO-based MTJs prepared using conventional sputtering on the annealing temperature. By annealing at 270 °C, the top amorphous CoFeB electrode began to crystallize locally at the interface between CoFeB and crystalline MgO barrier. The (100) plane of CoFeB at the MgO/CoFeB interface which is matched with MgO (100) lattice grows into amorphous CoFeB region. The increase in the MR ratio with annealing can be attributed to the formation of (100) crystalline structure of CoFeB well lattice matched with the (100)-oriented MgO barrier.

The authors gratefully acknowledge STMicroelectronics and the Data Storage Systems Center of Carnegie Mellon University for its financial support of the research project.

[1] S. A. Wolf, D. D. Awschalom, R. A. Buhrman, J. M. Daughton, S. von Molnar, M. L. Roukes, A. Y. Chtchelkanova, and D. M. Treger, Science **294**, 489 (2001).
[2] J. M. Daughton, J. Appl. Phys. **81**, 3758 (1997).
[3] W. H. Butler, X.-G. Zhang, T. C. Schulthess, and J. M. MacLaren, Phys. Rev. B **63**, 054416 (2001).
[4] J. Mathon and A. Umersky, Phys. Rev. B **63**, 220403(R) (2001).
[5] X.-G. Zhang and W. H. Butler, Phys. Rev. B **70**, 172407 (2004).
[6] S. S. Parkin, C. Kaiser, A. Panchula, P. M. Rice, B. Hughes, M. Samant, and S.-H. Yang, Nat. Mater. **3**, 862 (2004).
[7] S. Yuasa, T. Nagahama, A. Fukushima, Y. Suzuki, and K. Ando, Nat. Mater. **3**, 868 (2004).
[8] D. D. Djayaprawira *et al.*, Appl. Phys. Lett. **86**, 092502 (2005).
[9] J. Hayakawa, S. Ikeda, F. Matsukura, H. Takahashi, and H. Ohno, Jpn. J. Appl. Phys., Part 2 **44**, L587 (2005).
[10] D. A. Porter and K. E. Easterling, *Phase Transformations in Metals and Alloys*, 2nd ed. (Chapman and Hall, London, 1992), Chap. 4.
[11] J. Zhang and R. M. White, J. Appl. Phys. **83**, 6512 (1998).
[12] S. Zhang, P. M. Levy, A. C. Marley, and S. S. P. Parkin, Phys. Rev. Lett. **79**, 3744 (1997).